Nonlinear Contributions to the Frequency Spectrum of Wind-Generated Water Waves

G. J. KOMEN

Division of Oceanographic Research, Royal Netherlands Meteorological Institute, De Bilt, The Netherlands

(Manuscript received 7 September 1979, in final form 19 December 1979)

ABSTRACT

In the continuous frequency spectrum of wind-generated water waves Fourier components have different origins. At a particular frequency, some will be harmonics resulting from the nonlinear profiles of lower frequency waves, others will be near-free gravity waves. In this paper the relative importance of these two different contributions is studied in the case that the nonlinearities can be treated perturbatively. The calculation starts from a fit to observed spectra: in the sea the JONSWAP spectrum is chosen; in the laboratory a different fit with a sharper fall-off near the spectral peak is taken. The nonlinear corrections are most significant at frequencies larger than twice the peak frequency and increase with increasing frequency. They are determined mainly by the behavior of the spectrum near the peak. The relative importance of the nonlinear contributions increases with decreasing dimensionless fetch. This is in agreement with experimental observations. In the laboratory, with narrower spectra, nearly all of the spectral energy at twice the peak frequency is due to the nonlinear contributions. The observed magnitude agrees reasonably well with our calculated value. In the open-ocean nonlinear corrections are a small fraction of the linear contribution at this frequency. For a nonlinear system the concept of phase velocity loses its meaning in general. Nevertheless, experimentally, nonlinearities will show up as an anomaly in the observed phase velocity. This anomaly is studied. In the laboratory, where the nonlinearities dominate, a large anomaly is expected and this agrees with the observations. In the open sea experimental evidence is conflicting. It is found that several mechanisms tend to suppress the anomaly, so that small deviations from the linear value are obtained.

1. Introduction

A periodic nonlinear water wave is sharpened at the crests and flattened at the troughs. It can be viewed as a superposition of an infinity of discrete harmonics, bound to a fundamental wave.

In case of wind-generated waves one encounters a continuum of such nonlinear waves. Therefore, in a spectral analysis of a time record, high-frequency Fourier components can have different origins. Some will be harmonics resulting from the nonlinear profiles of lower frequency waves, others will be near-free gravity waves. Sometimes the harmonics are called bound waves to distinguish them from the fundamental waves. In this paper we intend to study the relative importance of the way in which bound waves and fundamental waves contribute to the wave spectrum.

Of course, it has to be realized that a bound wave is not a physical phenomenon in its own right. The concept arises when a Fourier analysis is made of the real motion at one position of a water surface. This analysis has its shortcomings because the Fourier modes, forming a complete basis of fundamental waves in the linear case, are somewhat artificial in the case of real nonlinear waves. Nevertheless, for weakly nonlinear systems the analysis in terms of Fourier modes is very useful because the nonlinearities can be treated as a perturbation.

The nonlinearities, in general, have two effects. One is a very weak interaction between the Fourier modes. This interaction is weak because it is not a first-order effect. It first occurs at second order as a resonant interaction arising from a secular term in the perturbation series. The slow interaction can have great dynamic significance and it has been studied in detail by several authors (Hasselmann, 1962; Fox, 1976; Webb, 1978). In this paper we address our attention to the other effect, namely the occurrence of bound waves. The first calculations on this were made by Tick (1959) even before the importance of resonant interactions had been realized. For weak nonlinearities both effects have their own characteristic time scale. Harmonic generation—or generation of bound waves as we call it—can take place in a few wave periods, whereas resonant interaction is not significant until after many periods.

0022-3670/80/050779-12$07.00

In practice, a wave field is analyzed with the help of the Fourier analysis of wave records. Such a record is chosen to cover a duration which is small with respect to changes in the spectrum, such as the secular change due to resonant interactions. Therefore, as far as the analysis is concerned, the spectrum can be considered stationary and the fundamental Fourier modes behave as free waves. In this way one consequence of the nonlinear nature is transferred from wave analysis to the domain of spectral evolution. Bound waves cannot be disposed of in this way. However, as we will see, a distinction between fundamental and bound waves is possible under certain conditions on theoretical grounds. An early indication of the presence of bound waves in the ocean came from HF backscatter measurements. There, in addition to the primary Bragg line which results from interaction with free waves, a second-order line was observed and it was explained as originating from a discrete higher order contribution to the wave spectrum (Crombie, 1955).

Our study has been motivated by measurements of the phase velocity of spectral components of wind-generated water waves in the laboratory (Ramamonjiarisoa and Coantic, 1976; Ramamonjiarisoa *et al.*, 1978; Mitsuyasu *et al.*, 1978; Lake and Yuen, 1978) and in the sea (Yefimov *et al.*, 1972, Ramamonjiarisoa and Giovanangeli, 1978). Deviations from the free phase velocity were found and it has been suggested that these indicate the presence of bound waves. Mitsuyasu *et al.* (1978 and 1979) and Masuda *et al.* (1979) have given a satisfactory explanation for their observed anomalous phase velocity. They used a perturbation method to calculate the nonlinear effects in their own observations. Here we will use a similar approach to study a wide class of spectra. This will enable us to discuss the importance of bound waves as a function of the parameters characterizing the wave spectrum, such as fetch and total wave energy.

The formalism is outlined in Sections 2–5. In Section 6 we give applications to the JONSWAP spectrum (Hasselmann *et al.*, 1973, 1976), which is consistent with many observed wave fields. In laboratory situations the JONSWAP fit seems less useful. Therefore, laboratory-generated waves are discussed separately in Section 7. Our conclusions are summarized in Section 8.

2. Definitions

We consider a one-dimensional, homogeneous and stationary distribution of weakly nonlinear, irrotational, deep-water waves, all moving in the same direction. The space-time correlation of the water height $\eta(x,t)$ is defined by

$$\tilde{P}(\xi,\tau) = \langle \eta(x+\xi, t+\tau)\eta(x,t)\rangle . \tag{1}$$

Its Fourier transform $P(k,\omega)$ is defined by

$$\tilde{P}(\xi,\tau) = \int_{-\infty}^{+\infty} dk \int_{-\infty}^{+\infty} d\omega e^{i(k\xi-\omega\tau)} P(k,\omega). \tag{2}$$

From the reality of η and the homogeneity of the wave field it follows that

$$P(k,\omega) = P^*(k,\omega) = P(-k,-\omega). \tag{3}$$

The assumption of weak nonlinearity makes it meaningful to introduce the zeroth-order spectrum P_0

$$P(k,\omega) = P_0(|k|)\delta(\omega - \sqrt{g|k|}) + P'(k,\omega) + (k \leftrightarrow -k,\ \omega \leftrightarrow -\omega), \tag{4}$$

where g is the gravitational constant. Since all waves move in the same direction, P can be taken to vanish unless k and ω have the same sign. Therefore, a one-sided wavenumber/frequency spectrum can be defined as

$$S(k,\omega) = \begin{cases} 2P(k,\omega), & k,\ \omega > 0 \\ 0, & \text{elsewhere.} \end{cases} \tag{5}$$

This implies the normalization

$$E \equiv \langle \eta^2 \rangle = \int_0^\infty dk d\omega S(k,\omega). \tag{6}$$

The total energy of the wave field equals $g\rho E$, where ρ is the water density. The frequency spectrum can be defined as

$$S(\omega) = \int_0^\infty dk S(k,\omega), \tag{7}$$

while wavenumber spectrum and cross spectrum are defined as

$$S(k) = \int_0^\infty d\omega S(k,\omega), \tag{8}$$

$$S(\omega,r) = \int_0^\infty dk e^{ikr} S(k,\omega). \tag{9}$$

For all of these spectra one may define

$$S = S_0 + S', \tag{10}$$

where

$$S_0(k) = 2P_0(k), \tag{11}$$

$$S_0(\omega) = \frac{4\omega}{g} P_0\left(\frac{\omega^2}{g}\right), \tag{12}$$

$$S_0(\omega,r) = S_0(\omega)e^{i\omega^2 r/g}. \tag{13}$$

Occasionally we will find it convenient to discuss results in terms of

$$\chi(\omega) = S'(\omega)/S_0(\omega), \tag{14}$$

which is a parameter characterizing the relative importance of the nonlinearities.

3. Perturbation results

From a perturbation expansion in the wave slope one can obtain an approximate expression for S' in terms of S_0. This approximation takes the form (Barrick and Weber, 1977)[1]

$$\left.\begin{aligned} S_1(k,\omega) &= \frac{k^2}{2g}\frac{\omega^2 - gk}{(2gk - \omega^2)^{1/2}} S_0(k_+)S_0(k_-) \\ k_\pm &= \frac{1}{2}\left[k \pm \frac{\omega}{g}(2gk - \omega^2)^{1/2}\right] \end{aligned}\right\} (gk)^{1/2} < \omega < (2gk)^{1/2} \tag{15a}$$

$$\left.\begin{aligned} &= \frac{k^2(g^2k^2 - \omega^4)}{4g\omega^3} S_0(k_+)S_0(k_-) \\ k_\pm &= \frac{1}{4g\omega^2}(gk \pm \omega^2)^2 \end{aligned}\right\} 0 < \omega < (gk)^{1/2} \tag{15b}$$

This expression is the lowest order, non-vanishing perturbation correction. It should be noted that in the same order of the perturbation expansion there is a small change in the energy on the free-wave dispersion surface. However, in this paper we will not consider this change. It is of some use to visualize the properties of $S_1(k,\omega)$ in the k,ω plane (Fig. 1). In general, S_1 is non-vanishing for $0 < \omega < (2gk)^{1/2}$ only. If, in addition, $S_0(k) = 0$ for $k < k_{\min}$, as is always the case in practice, then S_1 is nonzero in regions a and b only, i.e.,

$$k > 2k_{\min}, \quad \omega_{\min} + [g(k - k_{\min})]^{1/2} < \omega < (2gk)^{1/2}, \tag{16a}$$

$$0 < \omega < [g(k + k_{\min})]^{1/2} - \omega_{\min}, \qquad \omega_{\min} = (gk_{\min})^{1/2}. \tag{16b}$$

Therefore, to this order of perturbation theory there is a clear separation between the free waves at $\omega^2 = gk$ and the forced waves in the regions (a) and (b). These regions are indicated in Fig. 1 for the case $\omega_{\min} = \frac{1}{2}\omega_0$.

$S_1(k,\omega)$ peaks near the line $\omega = (2gk)^{1/2}$. In fact, it has a (kinematic) singularity on this line. This singularity is integrable and has no dynamical origin, unlike the additional peaking which may arise from the behavior of S_0. Normally S_0 is peaked sharply at some value of k, say, k_0. This then is reflected in a peaking of S_1 at

$$\left.\begin{aligned} &\text{I:} \quad \omega = \omega_0 + [g(k - k_0)]^{1/2}, \quad k > k_0, \quad \omega_0 = (gk_0)^{1/2} \\ &\text{II:} \quad \omega = \omega_0 - [g(k_0 - k)]^{1/2}, \quad k < k_0 \\ &\text{III:} \quad \omega = [g(k + k_0)]^{1/2} - \omega_0. \end{aligned}\right\} \tag{17}$$

These curves are parabolas with their symmetry axis parallel to the k axis; they are indicated in Fig. 1. Double peaking [i.e., peaking of both factors S_0 in Eq. (15)] occurs at $(k,\omega) = (0,0)$ and at $(k,\omega) = (2k_0,2\omega_0)$. It is readily seen that the secondary peak at $(2k_0,2\omega_0)$ dominates the nonlinear corrections, provided the peaking of $S_0(k)$ is sufficiently sharp. The low-frequency corrections have been studied by Tick (1963). In the following we will concentrate on the behavior of S_1 near the first harmonic, at $\omega = 2\omega_0$, which is the region of our main interest.

It is instructive to calculate S_1 for a few lowest order spectra. As a first example, we take a Dirac δ function for S_0

$$S_0(k) = Ak_0^{-2}\delta(k - k_0). \tag{18}$$

Substitution in (15a) gives a Stokes-like result

$$S_1(k,\omega) = Ak_0^{-2}\delta(k - 2k_0)\delta(\omega - 2\omega_0), \qquad \omega_0 = (gk_0)^{1/2}, \tag{19}$$

which leads to a cross-spectrum

$$S_1(\omega,r) = A^2g^2\omega_0^{-4} \times e^{(2i\omega_0^2r/g)}\delta(\omega - 2\omega_0), \tag{20}$$

which is periodic in space with a wavelength equal to one-half of the dominant wavelength.

A different simplified spectrum has been considered by Barrick and Weber (1977). They started from

$$S_0(k) = \begin{cases} \dfrac{A}{2k^3}, & k > k_0 \\ 0, & 0 < k < k_0, \end{cases} \tag{21}$$

[1] Note that our Eq. (15) has been corrected for two misprints, which appear in the formulas given in (24) and (25) of Barrick and Weber (1977). An error in their Eq. (28) is corrected in our Eq. (22).

which is a reasonable spectrum in the so-called saturation range. The following expression results:

$$S_1(k,\omega) = \begin{cases} \dfrac{2A^2g^5k^2}{(2gk-\omega^2)^{1/2}(\omega^2-gk)^5}, & k > 2k_0, \\ & \omega > 2\omega_0, \\ & \omega_0 + [g(k-k_0)]^{1/2} < \omega < (2gk)^{1/2}, \\ \dfrac{64A^2g^5\omega^9k^2}{(g^2k^2-\omega^4)^5}, & \omega < [g(k+k_0)]^{1/2} - \omega_0 \\ 0, & \text{elsewhere.} \end{cases} \tag{22}$$

For $\omega \sim 2\omega_0$ this yields the following result for the cross-spectrum:

$$S_1(\omega,r) \approx \frac{16A^2g^2}{\omega^6}(\pi g/r)^{1/2}e^{i\omega^2r/2g}[C(d) + iS(d)],$$
$$d = (\omega - 2\omega_0)(r/2g)^{1/2}, \tag{23}$$

where C and S are the Fresnel integrals. Note again that $S_1(\omega,r)$ is periodic in space with a wavelength equal to one-half of the dominant value, albeit, with a slowly varying amplitude.

From both examples we see that a lowest order peak at (k_0,ω_0) leads to a secondary peak near $(2k_0,2\omega_0)$. This peak results in a (near) periodic behavior of the corresponding cross-spectrum.

4. Phase velocities

A phase velocity can be defined when there exists a definite relationship between the wavelength and the wave period. In the linear, deep-water case

$$c = \omega/k = (g/k)^{1/2} = g/\omega. \tag{24}$$

The nonlinear corrections discussed above, do not, in general, allow for the definition of a phase velocity, as was stressed by Tick (1959). However, if $S_1(k,\omega)$ is sharply peaked in a small region of the (k,ω) plane, say, around (k_p,ω_p), an approximate velocity can be defined as

$$c_1 = \omega_p/k_p. \tag{25}$$

Obviously, this definition works for the discrete spectrum of Eq. (19). One finds

$$c_1 = \omega_0/k_0 = g/\omega_0 \tag{26}$$

as expected, because in the discrete case the nonlinear corrections define a steady modification of the fundamental wave with wavenumber k_0. The same value for the phase velocity is obtained in the example of Eq. (22), where S_1 peaks near $(2k_0,2\omega_0)$.

An alternative definition for the phase velocity can be given from the behavior of the cross spectral density. This definition,

$$c(\omega) = \frac{\omega r}{\arctan(\mathrm{Im}S(\omega,r)/\mathrm{Re}S(\omega,r))}, \tag{27}$$

is used in practice to calculate phase velocities from an experimental determination of the cross spectrum. In the linear case, this definition is independent of r and coincides with the definition given in (24), as can be verified when (13) is substituted into (27).

Taking $r \to 0$ in (27), the definition of c can be applied in nonlinear situations, although, in general, c loses its meaning in this case as a phase velocity. However, in the cases where a phase velocity can be defined, as in (25), it can be checked that Eqs. (27) and (25) are consistent. This is easily understood because strong peaking in the (k,ω) plane implies approximate periodicity of the cross spectrum. This is best illustrated with Eq. (23) which can be written as

$$S_1(\omega,r) = f(\omega,r)e^{i\omega^2r/2g}, \tag{28}$$

where f is a slowly varying function of r. Applying (27) to (28) we find

$$c = 2g/\omega, \tag{29}$$

which for $\omega = 2\omega_0$ agrees with (26).

When, for a given ω, $S(k,\omega)$ peaks for several values of k (e.g., $gk = \omega^2$ and $2gk = \omega^2$) the definition (27) loses its physical meaning. Nevertheless, Eq. (27) has been used for the analysis of nonlinear data. It is therefore interesting to see what one may expect from such an analysis when several peaks are present. As an example, we consider the case where $S(k,\omega)$ is peaked for $\omega = 2\omega_0$ at $k = 4k_0$ (free waves) and at $2k_0$ and $8k_0$ (nonlinear waves in regions (a) and (b) of Fig. 1, respectively). This case is encountered in Section 6. If the nonlinear peaks are sufficiently narrow, the cross spectrum behaves as

$$S(\omega,r) = S_0(\omega)e^{ikr} + A(\omega,r)e^{ikr/2} + B(\omega,r)e^{2ikr},$$
$$\omega \approx 2\omega_0, \quad \omega^2 = gk, \tag{30}$$

with A and B slowly varying as functions of r. $A(\omega,0)$ and $B(\omega,0)$ measure the relative contribution of the nonlinear corrections to the spectrum from regions (a) and (b). Analyzing the individual terms of

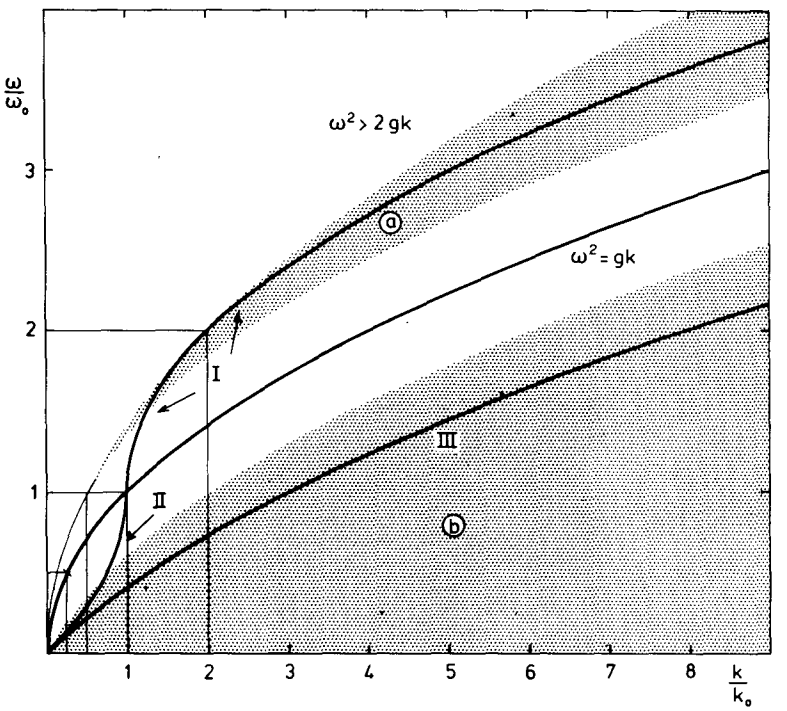

FIG. 1. Linear deep water waves contribute to the wavenumber/frequency spectrum along the line $\omega^2 = gk$ only. The nonlinear corrections, as given by Eq. (15), are non-vanishing in the regions ⓐ and ⓑ. It has been assumed that the spectrum peaks at (k_0,ω_0) and, for the sake of illustration only, that there is a lowest frequency at $\omega_{\min} = \frac{1}{2}\omega_0$ in the linear spectrum. The function S_1 is peaked on the lines I, II and III [cf. Eq. (17)].

(30) with (27) we find for $\omega \approx 2\omega_0$ that

$$\left.\begin{aligned} c_{\text{free}} &= \tfrac{1}{2}c_0 = c' \\ c_a &= c_0 = 2c', \quad c_0 = g/\omega_0 \\ c_b &= \tfrac{1}{4}c_0 = \tfrac{1}{2}c', \quad c' = g/2\omega_0 \end{aligned}\right\} . \tag{31}$$

These quantities have some physical significance in that they indicate the occurrence of three types of Fourier modes, each characterized by a specific propagation velocity. Taking all terms together one obtains from (27)

$$\left.\begin{aligned} c &= \frac{1 + \chi_a(\omega) + \chi_b(\omega)}{1 + \tfrac{1}{2}\chi_a(\omega) + 2\chi_b(\omega)} \frac{g}{\omega}, \quad \omega \approx 2\omega \\ \chi_{a,b} &= \frac{(A(\omega,0),B(\omega,0))}{S_0(\omega)} . \end{aligned}\right\} \tag{32}$$

The deviations from linear behavior are determined by the magnitude of χ_a and χ_b. As it happens, the deviation can be suppressed, because the contributions from regions ⓐ and ⓑ have an opposite effect on c. When $\chi_a = 2\chi_b$ the suppression is complete. Therefore, nonlinearities do not necessarily show up as an anomaly in the phase velocity, although in general they will lead to a deviation from the value for free waves.

5. The frequency spectrum

It is standard practice to determine frequency spectra from wave measurements. From the foregoing discussion it follows that these frequency spectra contain contributions from fundamental waves, satisfying $\omega^2 = gk$, as well as from bound waves. In order to separate these, we propose to calculate S_1 in an iterative way, as follows:

$$\left.\begin{aligned} &S_0^{(i)}(\omega) \to S_1^{(i)}(\omega), \quad i = 1, 2 \ldots, \\ &S_0^{(1)} = S, \quad S_0^{(i+1)} = S - S_1^{(i)} \end{aligned}\right\} \tag{33}$$

where S is the measured frequency spectrum. It is important that realistic wave spectra behave in the way we discussed in Section 4, i.e., S_0 peaks at $\omega = \omega_0$, while S_1 peaks at twice this frequency. Further, it is important that the magnitude of S_1 near $\omega = 2\omega_0$ is determined by the value of S_0 at $\omega = \omega_0$, because this leads to a rapid convergence of the iterative scheme. In the following we will make one iteration only, since this leads to reasonable accuracy in most cases. To obtain $S_1^{(i)}$ from $S_0^{(i)}$ we must use Eq. (15), where for a given value of ω we have to integrate over all k. For later use it is convenient to derive an expression for the cross-spectrum $S(\omega,r)$. This is the Fourier transform of

(15) and for $r = 0$ this reduces to the frequency spectrum. Introducing a transformation of the integration variable, and expressing $S_0(k)$ in terms of $S_0(\omega)$, the resulting integral can be simplified and we find

$$S_1(\omega,r) = \frac{1}{2g^2}\int_{\omega/2}^{\infty} d\omega' \exp\{ir[\omega'^2 + (\omega-\omega')|\omega-\omega'|]g^{-1}\} \times [K(\omega',\omega) + K(\omega-\omega',\omega)] \times S_0(\omega')S_0(|\omega'-\omega|), \quad (34)$$

$$K(\omega',\omega) = \begin{cases} \omega'^2(\omega^2 - 2\omega\omega' + 2\omega'^2), & 0 < \omega' < \omega \\ (\omega - 2\omega')^2\omega\omega', & 0 < \omega < \omega'. \end{cases}$$

This is essentially equivalent to Tick's (1959) result. It is convenient to scale the quantities involved. This is often done by scaling the spectrum with respect to the total energy. Here we find it more convenient to scale with respect to the value of the spectrum at the peak. [For a given spectral shape the energy and the peak value are simply proportional; in fact, from Mitsuyasu (1968), $E \approx S(\omega_0)\omega_0$.] Defining

$$s(x) = S(\omega_0 x)/S(\omega_0), \quad x = \omega/\omega_0, \quad (35)$$

we obtain for the first-order nonlinear correction to the frequency spectrum

$$s_1(x) = \frac{S_0(\omega_0)\omega_0^5}{2g^2}\int_{x/2}^{\infty} dx'[K(x',x) + K(x-x',x)] \times s_0(x')s_0(|x-x'|). \quad (36)$$

We will use this equation in the recursive scheme (33) to analyze fits to observed spectra for their nonlinear content. The factor $S_0(\omega_0)\omega_0^5$ has a physical interpretation. It is proportional to the square of the significant wave steepness $H_{1/3}/L_{1/3}$. This can be easily seen. The significant wave height $H_{1/3}$ squared is proportional to the total energy, and this in turn is proportional to $S(\omega_0)\omega_0$. The significant wavelength $L_{1/3}$ is proportional to ω_0^{-2}. It is not surprising that the importance of the nonlinear corrections is determined by the wave steepness, since this is the parameter in which the perturbation expansion leading to (15) has been made: steeper waves are more nonlinear.

6. Application to the JONSWAP spectrum

It is claimed (Hasselmann *et al.*, 1976) that the majority of observed spectra of wind-generated waves agrees well with the functional form

$$S_J(\omega) = \frac{\alpha g^2}{\omega^5}\exp\left[-\frac{5}{4}\left(\frac{\omega_0}{\omega}\right)^4 + (\ln\gamma)\exp\left(-\frac{(\omega-\omega_0)^2}{2\sigma^2\omega_0^2}\right)\right]$$

$$\sigma = \begin{cases} \sigma_l, & \omega < \omega_0 \\ \sigma_r, & \omega > \omega_0. \end{cases} \quad (37)$$

In this five-parameter fit the parameters α and ω_0 have been correlated with the fetch X:

$$\left.\begin{aligned} \alpha &= 0.076\xi^{-0.22}, \quad \xi = gX/U^2 \\ U\omega_0/g &= 22\xi^{-0.33} \end{aligned}\right\}. \quad (38)$$

Here U is the wind velocity at 10 m height above sea. The remaining parameters, σ_l, σ_r and γ, show no clear correlation with fetch. The average JONSWAP values are $\gamma = 3.3$, $\sigma_l = 0.07$ and $\sigma_r = 0.09$.

It is important to note that the parameters in (37) were determined from a fit to data for $\omega < 2\omega_0$. For the present discussion it is convenient to assume that (37) holds up to at least three times the peak frequency. For $1 \ll \omega/\omega_0 \ll 2c_0/u_* = 2g/(u_*\omega_0)$ [$u_*^2 = \tau/\rho$ with τ the wind stress at the surface, $u_*^2 = C_D U^2$, $C_D \approx 10^{-3}$], Phillips (1978) assumed the existence of a saturation range. In this range the spectrum is proportional to ω^{-5}, so that the JONSWAP fit may be extended into this range. The drift velocity in the wind-drift layer is proportional to u_*, and c_0/u_* is therefore an important physical parameter. It can be related to the dimensionless fetch with the help of (38). For $C_D \approx 10^{-3}$ we find

$$c_0/u_* = 1.44\xi^{0.33} \quad (39)$$

and as a consequence the assumption that (37) holds for $\omega/\omega_0 \lesssim 3$ is reasonable for $\xi \gtrsim 10$.

To separate free waves and bound waves we can use Eq. (36) with

$$s_0(x) = \frac{1}{\gamma x^5}\exp\left[-\frac{5}{4}\left(\frac{1}{x^4} - 1\right) + \ln\gamma e^{-(x-1)^2/2\sigma^2}\right]. \quad (40)$$

from Eq. (37). This leads to one of our main results, namely,

$$s_1(x) = \xi^{-0.22}\gamma f(x;\gamma,\sigma). \quad (41)$$

The function f, which can be calculated numerically, is plotted in Fig. 2. With the help of this figure the magnitude of the nonlinear contribution to the frequency spectrum can be determined. An example is given in Table 1, where $\chi_J = 100[S_1(\omega)/S_J(\omega)]$ is shown for $\sigma_l = \sigma_r = 0.1$, $\gamma = 3$, for several frequencies and for different values of the dimensionless fetch. The values clearly illustrate the increasing importance of nonlinearities with decreasing dimensionless fetch and with increasing frequency. We will comment on each of these trends.

a. The frequency dependence

We first consider a fixed fetch, not too small, i.e., $\xi \gtrsim 10$. In the region $2\omega_0 < \omega < 3\omega_0$ the relative magnitude of the nonlinear contribution to the total spectrum ranges from a few to several tens of percents. Since by assumption the total spectrum is

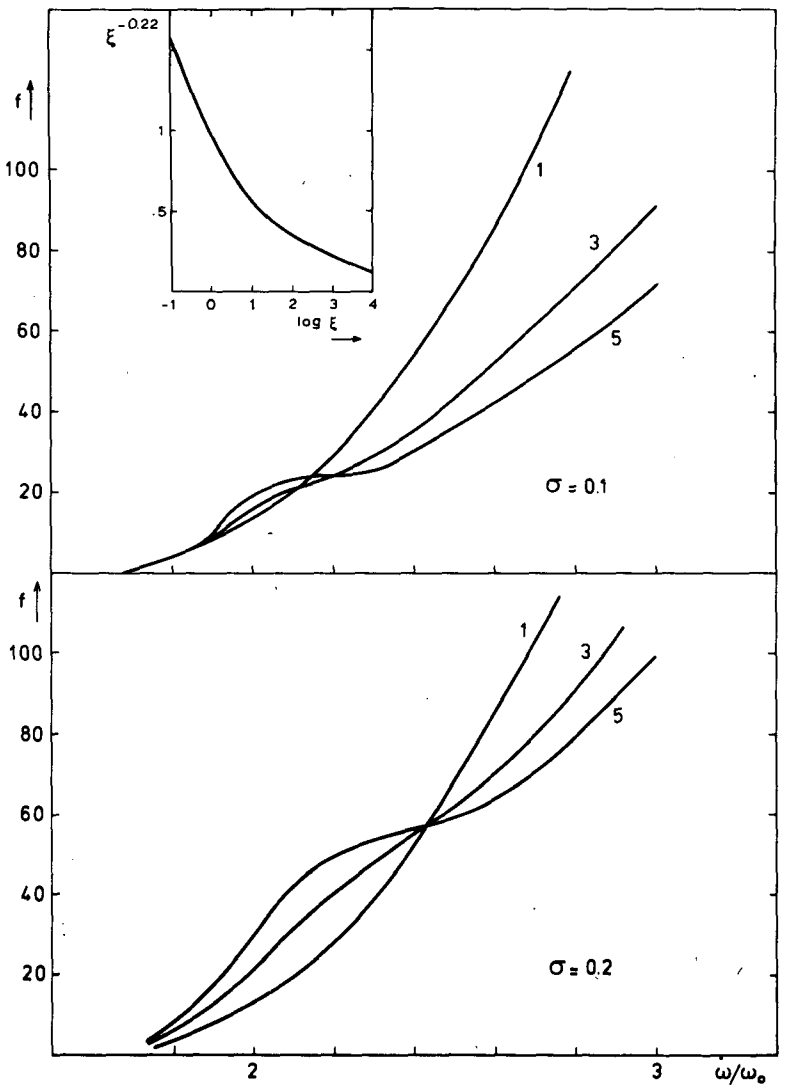

FIG. 2. The function f of Eq. (41), for several values of the JONSWAP parameter σ (upper and lower illustration) and γ (1, 3 or 5). With the help of the inset nonlinear corrections to the frequency spectrum can be estimated as a function of the dimensionless fetch $\xi = gX/U^2$.

JONSWAP, the contribution of free waves can be estimated by subtracting the values of Table 1 from 100%. We have made only one iteration but this should be a good approximation, since S_1 is mainly determined by the value of S_0 near the peak, while, in turn, the value of S_1 near the peak is completely negligible (cf. Fig. 2).

To get a rough idea of the accuracy of the approximation we have repeated the calculation starting from a different zeroth-order spectrum, namely, one with free waves totally absent for $\omega > 2\omega_0$, but JONSWAP otherwise. From the results, which are given in parentheses in the table, one gets an estimate of the error made by stopping after one iteration. For $\omega \approx 2\omega_0$ the error is of the order of 20%. For $\omega = 2.8\omega_0$ the errors become larger, because then a significant portion of S_1 is determined by the high-frequency behavior of S_0. It would be straightforward to improve the accuracy by performing a few more iterations, but this is not meaningful because at the higher frequencies the total spectrum is not known to sufficient accuracy.

TABLE 1. $S_1(\omega)/S_J(\omega) \times 100$ as a function of the dimensionless fetch $\xi = gX/U^2$. The linear part of the spectrum has been identified with the JONSWAP spectrum, i.e., $S_0 = S_J$. The figures in parentheses are obtained when $S_0 = S_J$, $\omega < 2\omega_0$; otherwise $S_0 = 0$ is chosen.

$\log\xi$	−1	0	1	2	3	4
c_0/u_*	0.7	1.4	3.1	6.6	14	30
ω/ω_0						
2.0	75 (60)	45 (36)	27 (22)	16 (13)	10 (8)	6 (5)
2.2	121 (96)	73 (58)	44 (35)	27 (21)	16 (13)	10 (8)
2.4	176 (139)	106 (84)	64 (51)	38 (30)	23 (18)	14 (11)
2.6		153 (121)	92 (73)	56 (44)	33 (26)	20 (16)
2.8			126 (97)	76 (58)	46 (35)	28 (21)
3.0				99 (53)	60 (32)	36 (19)

b. Fetch dependence

From Eq. (41) it can be seen that for decreasing ξ the nonlinearities increase like $\xi^{-0.22}$. For $\xi \approx 10$ the JONSWAP spectrum ceases to be a good fit. At the corresponding small values of c_0/u_* the physics changes as microscale breaking, caused by the relatively strong surface drift, starts to eliminate free waves at high frequencies. At small fetches, therefore, the numbers in Fig. 1 lose their physical meaning. Nevertheless, it is instructive to see just how significant such increasing nonlinearities are. At $\omega = 2.6\omega_0$ and $\xi = 1$ the nonlinearities exceed the JONSWAP value, and this results in a breakdown of the recursive scheme. As a consequence, a spectrum which for $\xi = 1$ is JONSWAP for $\omega < 2\omega_0$ cannot be JONSWAP for $\omega \geq 2.6\omega_0$. In the next section we will consider a fit which is more realistic in laboratory situations.

It is not so hard to find a qualitative understanding of the decrease of χ_J, when ξ increases. The factor $S_0(\omega_0)\omega_0^5$ in Eq. (36) is a measure for the steepness of waves with a frequency $\omega \approx \omega_0$. With increasing fetch this factor decreases, the profiles of the fundamental waves become less nonlinear, and as a consequence bound waves will have less influence on the frequency spectrum at $\omega \approx 2\omega_0$.

c. Phase velocities

For medium to long dimensionless fetches the results of Table 1 suggest the presence of small but non-negligible nonlinear corrections for frequencies higher than twice the peak frequency. Experimentally, there is little known about nonlinearities in this range, for $c_0/u_* \geq 10$. Information on the full wavenumber/frequency spectrum is completely lacking, but several investigators (Yefimov *et al.*, 1972; Ramamonjiarisoa and Giovanangeli, 1978) have measured spatial correlations in this frequency range, and from these phase velocities have been calculated. Near the spectral peak deviations from g/ω are generally small (~20%) and explainable in terms of angular spread and Doppler shift caused by the wind drift layer. For higher frequencies the observed deviations are larger, although the exact size varies considerably from measurement to measurement. Theoretically, starting from the JONSWAP spectrum a small anomaly is expected. Taking, as an example, $\chi_a \approx 20\%$ and $\chi_b = 0$ [cf. Eq. (32)] an anomaly of only 10% would follow. The contributions from region b would lead to a further reduction, since the suppression mechanism described in the text following Eq. (32) seems to be operative. We find $\chi_b = 0.2\chi_a$ and this would reduce the anomaly to only 3%.

Unfortunately, the experimental results have been obtained from wave fields which have not been described in terms of JONSWAP spectra, so that a comparison with our results is not easy. However, a few comments can be made. Yefimov *et al.* (1972) made measurements 300 m off the coast of the Black Sea under variable meteorological conditions, whereas a value of ξ was not given. They estimate the net excess of the phase velocity over the linear value (at $2\omega_0$) at 30%. In view of the foregoing remarks this is surprisingly large. Neglecting contribution from (b), it would require $\chi(2\omega_0) \approx 100\%$. In two measurements Ramamonjiarisoa *et al.* (1978) obtained small deviations from the free phase velocity, which is consistent with our theoretical expectations. In one other measurement results were obtained that were compatible with those of Yefimov. It would be interesting to see if the large anomalies can be accounted for with an iterative approach starting from a precise fit to the observed spectra. Such a calculation is outside the scope of the present paper, however.

7. Spectra describing laboratory situations

The difference in dynamics of wind waves in the laboratory and in the sea has been stressed by Phillips (1977, 1978). An important parameter characterizing this difference is c_0/u_*, a measure for the ratio of the phase velocity of waves at the spectral peak and the velocity in the wind-drift layer. When c_0/u_* is of the order 1, which corresponds to small dimensionless fetch, the importance of small-scale breaking is strongly enhanced. As a consequence, observed spectra fall off very rapidly away from the spectral peak. Often a secondary peak is observed at twice the peak frequency. Examples of observed spectra are given by Mitsuyasu (1968), Hidy and Plate (1966), Ramamonjiarisoa and Coantic (1976) and Lake and Yuen (1978). The JONSWAP fit fails to describe the detailed structure of these spectra. In this section we suggest a simple fit to the observed behavior near the spectral peak. With this fit as an input to the recursive scheme we then calculate the nonlinear corrections for higher frequencies.

The fit we suggest near the spectral peak is

$$S(\omega) = \begin{cases} \kappa\left(\dfrac{\omega_0}{\omega}\right)^{n_r}, & \omega_0 < \omega \leq 1.6\omega_0, \\ \kappa\left(\dfrac{\omega}{\omega_0}\right)^{n_l}, & 0.6\omega_0 \leq \omega < \omega_0, \end{cases} \tag{42}$$

or in terms of the scaled spectrum [Eq. (35)]

$$s(x) = \begin{cases} x^{-n_r} & 1 < x \leq 1.6, \\ x^{n_l} & 0.6 \leq x < 1. \end{cases} \tag{43}$$

We will not attempt to explain the observed values of n_r and n_l, which are found to lie in the range between 7 and 13, or κ, which is the magnitude of the

frequency spectrum at the peak. Instead we will use observed values as an input for our calculations. The data indicate a considerable variability in the value of κ. From Ramamonjiarisoa and Coantic (1976) and Mitsuyasu (1968) we would infer κ to be of the order of 10^{-5} m^2 s. Unfortunately, Lake and Yuen (1978) do not give their absolute normalization, so that a determination of κ from their data is not possible. In the following we will always take $\kappa = 3 \times 10^{-5}$ m^2 s as derived from Ramamonjiarisoa and Coantic [1976 (case $U = 8$ m s^{-1}].

Of course, our fit is a schematic one, and very rough especially at the peak frequency. In addition to the "triangular fit" (in the $\ln S - \ln\omega$ plane) we have considered a "trapezoid fit," where the apex of the triangle was replaced by a small, horizontal line element. This did not lead to substantial changes in our conclusions. Here we will report results for the triangular fit only, so as to avoid the introduction of additional free parameters.

It is straightforward to calculate the nonlinear corrections from Eq. (36), which take the form

$$s_1(x) = \frac{\kappa\omega_0^5}{2g^2}\int_{x/2}^{\infty} dx'[K(x',x) + K(x - x', x)] \times s_0(x')s_0(|x - x'|). \quad (44)$$

The peaking of the laboratory spectra [Eq. (42)] is more pronounced than that of the JONSWAP spectrum. As a consequence the contribution from region b in Fig. 1 turns out to be negligible in the laboratory. The dominant contribution comes from a, where the integrand in (44) peaks doubly. In practice this means that for $x \approx 2$, the integral can be cut off at $x' = 2$, when for s_0 we take s of Eq. (43) extended to $x > 1.6$.

It is instructive to do a rough analytic calculation first. This can be done for $x = 2$. Approximating the K functions [Eq. (34)] by their values at $x' = 1$ and taking $n_l = n_r = n$, we obtain the simple integrable expression

$$s_1(2) = \frac{4\omega_0^5\kappa}{g^2} I_n, \quad I_n = \int_0^1 dz \frac{z^n}{(1 + z)^n}, \quad (45)$$

where I_n can be shown to equal

$$I_n = -\tfrac{1}{2} + (-1)^n\left[1 - \tfrac{1}{2} + \tfrac{1}{3} + \cdots (-1)^n \frac{1}{n-1} - \ln 2\right]n. \quad (46)$$

Choosing $n = 10$, $\omega_0 = 4\pi$ and $\kappa = 3 \times 10^{-5}$ m^2 s, which are reasonable values, we find $I_{10} = 0.025$ and

$$s_1(2) \approx 0.01. \quad (47)$$

Comparing this with

$$s_0(2) = \frac{1}{2^{10}} \approx 0.001, \quad (48)$$

we see that the nonlinearities exceed the linear part of the spectrum at this frequency by one order of magnitude.

In Fig. 3 we have plotted both s_0 and $s_0 + s_1$ for several values of n_r; n_l has been chosen as -12.5 to fit the rapid fall-off at low frequencies. The plot is based on a numerical evaluation of Eq. (44). It shows how the relative importance of the nonlinearities near the harmonic peak grows when n_r increases. The spectra observed by Ramamonjiarisoa and Coantic (1976) seem to be closest to the case $n_r = 7.5$. Their data fall within the band indicated in Fig. 3. For $n_r = 7.5$ we have $s_0 + s_1 = 0.017$ at the harmonic peak, while the observed value is roughly 10^{-2}. We think that this is a reasonable agreement, given the roughness of our fit. The spectra reported by Lake and Yuen (1978) show a steeper high frequency face, $n_r \approx 11.5$, and a more pronounced harmonic peak. This is in accord with our Fig. 3. A quantitative comparison cannot be made, because the experimental normalization is not available.

Ramamonjiarisoa and Coantic (1976) investigated how the frequency spectra depend on the dimensionless fetch $3 \leqslant \xi \leqslant 10$. Their results for different fetches were plotted in a double logarithmic plot, in a scaled form, i.e., $S(\omega)\omega_0/E$ is given as a function of ω/ω_0. Spectra presented in this way seem to be independent of the dimensionless fetch, not only near the spectral peak, but also near the first harmonic. This scaling behavior is quite surprising at first sight, since roughly, $S'(2\omega_0)$ is determined by $S(\omega_0)$ squared and this depends on the dimensionless fetch. However, it can be understood with the help of Eqs. (42) and (44) and with the independent observation (Mitsuyasu, 1968) that the wave steepness is approximately constant for all wind waves at short fetch. First, note that scaling near the spectral peak is obvious, because, for fixed n_r and n_l, $E \approx \kappa\omega_0$, so that

$$S(\omega)\omega_0/E \approx s(x) \quad (49)$$

which is independent of κ. Next, to demonstrate scaling near the first harmonic, we have to show that the factor $\kappa\omega_0^5$ in Eq. (44) scales. This factor is proportional to the significant wave slope squared, as we discussed in the text following Eq. (36). In general, this wave slope depends on the dimensionless fetch ξ. However, from Mitsuyasu (1968) it follows that this dependence is small, and therefore

$$\kappa\omega_0^5 = \text{constant} \quad (50)$$

to a fair approximation. Using this in Eq. (44) the

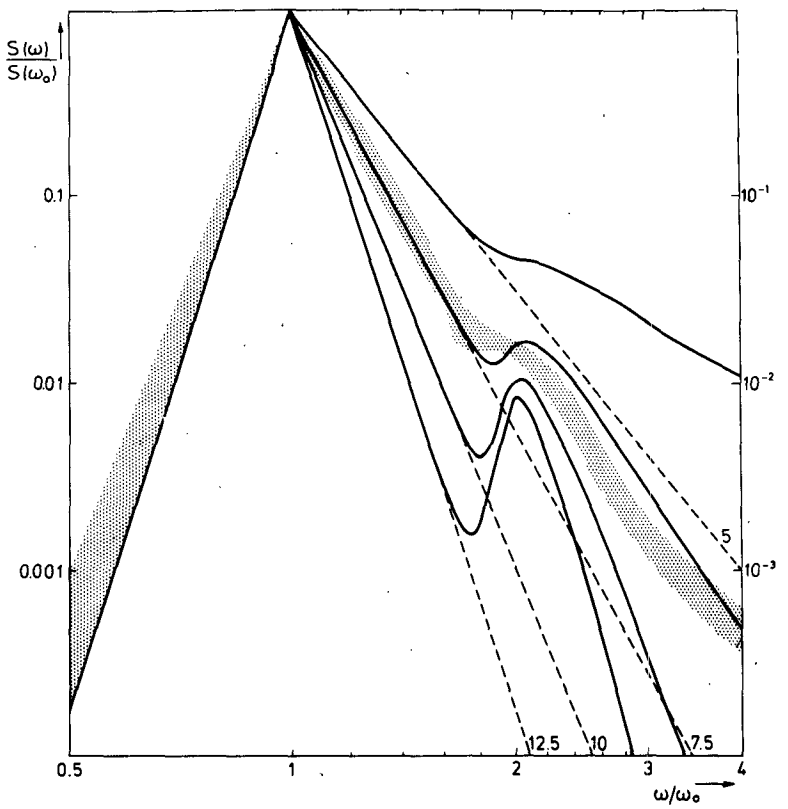

FIG. 3. $s_0 + s_1$ (solid line) and s_0 (dotted line) as a function of ω/ω_0 for the fit of Eq. (42) to laboratory spectra. $n_1 = 12.5$; the values of n_r label the various curves. The fetch-limited data of Ramamonjiarisoa and Coantic (1976) all fall within the shaded band.

scaling of the nonlinear corrections follows. Note that our scaling arguments are valid for given slope parameters (n_r,n_l). It seems that n_r increases for extremely short fetches ($\xi \lesssim 1$) such as those considered, e.g., by Lake and Yuen (1978). Obviously, the scaling property is lost in this case.

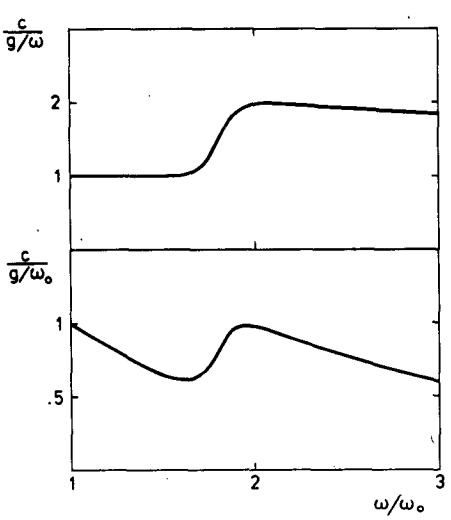

FIG. 4. The phase velocity c calculated from the definition equation (27), starting from Eq. (42), with $n_r = n_l = 12.5$.

Finally, we would like to consider the influence of the nonlinear corrections on the phase velocity measurements, such as have been reported by Ramamonjiarisoa and Coantic (1976) and Lake and Yuen (1978). Using the definition of Eq. (27), we have calculated the phase velocity for the spectrum (42). The result is given in Fig. 4 for the somewhat extreme case $n_r = n_l = 12.5$. There is a clear deviation from the linear value, which sets in at twice the peak frequency, the calculated value being twice the linear one, and equal to the phase speed of the dominant waves. It represents the nonlinear modification of the profiles of the dominant waves, and is exactly twice the free value because the free waves at twice the peak frequency are strongly suppressed [$\chi^{-1}(2\omega_0) \equiv S_0(2\omega_0)/S_1(2\omega_0) \approx 2\%$] and the nonlinear contributions from regions other than $(\omega,k) \approx (2\omega_0,2k_0)$ are completely negligible. Of course, Fig. 4 corresponds to an extreme spectrum. In less extreme cases the anomaly is less pronounced. To give a few examples: for $(n_l,n_r) = (12.5, 10)$ we find $\chi^{-1}(2\omega_0) = 11\%$ and $c(2\omega_0) = 0.9c(\omega_0)$, while for $(n_l,n_r) = (12.5, 7.5)$, which

is closer to the spectra reported by Ramamonjiarisoa and Coantic (1976), we find $\chi^{-1}(2\omega_0) = 53\%$ and

$$c(2\omega_0) = 0.75c(\omega_0). \quad (51)$$

In the latter case the contributions from regions other than $(k,\omega) \approx (2k_0,2\omega_0)$ are still quite small, of the order of 1% of the nonlinear part. This has to be compared with the 20% obtained for waves in the sea (see Section 6c). Eq. (51) does not fully explain the observed value $c_{obs}(2\omega_0) = c(\omega_0)$, $\omega > 2\omega_0$. It is very likely that the 30% discrepancy can be accounted for by the effects of surface drift and angular spread.

For $\omega < 2\omega_0$ we do not find a significant nonlinear effect. Therefore the anomaly sets in at $\omega \approx 2\omega_0$, as in Fig. 4. This is not inconsistent with the results of Ramamonjiarisoa and Coantic (1976). The onset of the anomaly is expected to be sharper in the data of Lake and Yuen (1978), because their spectra peak more sharply. It is surprising, therefore, that their reported phase velocity is a constant over the whole range of values $\omega > \omega_0$. This result cannot be explained by our perturbative calculation.

8. Conclusion

In the spectral analysis of a single nonlinear water wave one finds a fundamental contribution at (k_0,ω_0) and harmonics, the first of these at $(2k_0,2\omega_0)$. In the case of wind-generated waves one has a continuum of Fourier modes, which, as in the discrete case, one would like to distinguish in fundamental and harmonic contributions. We have tried to make a few general conclusions about the way in which this distinction can be made. We restricted ourselves to weak nonlinearities and based our study on a perturbative scheme, which started from simple fits to observed spectra.

In the continuum case, we found the distinction between fundamental waves and bound waves can still be made. Fundamental waves are approximately free and satisfy the free dispersion relation $\omega^2 = gk$. Bound waves, which are the continuum generalization of the discrete harmonics, do not satisfy this relation. The condition that a distinction can be made is the occurrence of an infrared cutoff in the wave spectrum, because this led to the vanishing of $S'(k,\omega)$ in the neighborhood of $\omega^2 = gk$. In practice this condition is always satisfied. Normally, the wave spectrum peaks at a particular value (ω_0,k_0). The bound-wave contribution to the spectrum then peaks near $(2\omega_0,2k_0)$ in region a of Fig. 1. This can be seen as a generalization of the discrete result. However, for $\omega \approx 2\omega_0$ there is a secondary peak near $k = 8k_0$ (in region b of Fig. 1), which has no analogue in the discrete case.

These results are in agreement with the results from HF backscatter experiments (Barrick, 1978). There one finds a sharp first-order Bragg line, with a Doppler shift given by the linear dispersion relation; a relatively unimportant background corresponding to the bound wave continuum; and a secondary peak which corresponds to the harmonic peaking of the bound wave continuum. Our results bring together the original explanation by Crombie (1955) for this secondary peak, and the work of Hasselmann (1971) which concentrated on the continuum contribution.

The magnitude of the bound-wave contribution to the frequency spectrum can be given as a fraction of the peak value [cf. Eq. (35)] or equivalently as a fraction of the (total wave energy multiplied by ω_0). This quantity is found to be proportional to the product of the peak value of the frequency spectrum and the fifth power of the peak frequency [Eq. (36)] or the significant wave slope squared. In general, this wave slope—and therefore the importance of bound waves—decreases with increasing dimensionless fetch. This has been illustrated for the JONSWAP spectrum. In Table 1 the magnitude of the nonlinear contribution is given as a fraction of the linear contribution. The effect increases with increasing frequency. For $\omega > 2.6\omega_0$, however, our estimate becomes less reliable for reasons that have been explained in Section 6. For not too small dimensionless fetches, effects are of the order of 10%. Nonlinear anomalies in measured phase velocities are suppressed at least by a factor of 2 [cf. Eq. (32)]. An even stronger suppression may occur because of the delicate interplay of contributions from regions a and b (Fig. 1).

In the laboratory, the JONSWAP fit loses its applicability. For extremely short fetches ($c/u_* < 10$) a significant feature of wave spectra is the rapid fall-off of the spectrum just above the peak. The harmonic peak, frequently observed, reflects the absence of free waves. We have shown that the magnitude of the observed harmonic peak is in reasonable agreement with what we calculate, starting from the behavior of the spectrum near the peak. If the free waves fall off sufficiently fast, bound waves dominate completely for $\omega > 1.7\omega_0$.

The results of laboratory measurements are sometimes presented in dimensionless form $[\omega_0 S(\omega_0)/E$ vs $\omega/\omega_0]$. These laboratory results then seem to scale, independent of fetch. This scaling behavior can be understood as a consequence of the approximate fetch independence of the significant wave slope.

In the laboratory the dominance of bound waves at the harmonic peak leads to a clear anomaly in the phase velocity for $\omega \geq 1.7$ (cf. Fig. 4). At lower frequencies no anomaly is found.

Our application of simple perturbation results to realistic spectra could be extended to include the directional dependence as well as higher frequencies.

For general conclusions these extensions are useful only when experimental information is available, especially for the larger fetches, where virtually nothing is known about the high-frequency content of the spectrum.

Acknowledgments. I would like to thank my colleagues in the Division of Oceanographic Research of KNMI for discussions, especially Mr. E. Bouws and Prof. R. Dorrestein.

REFERENCES

Barrick, D. E., 1978: Hf radio oceanography—a review. *Bound.-Layer Meteor.*, **13,** 23–43.

——, and B. L. Weber, 1977: On the nonlinear theory for gravity waves on the ocean's surface. Part 2: Interpretation and applications. *J. Phys. Oceanogr.*, **7,** 11–21.

Crombie, D. D., 1955: Doppler spectrum of sea echo at 13.56 Mc./s. *Nature*, **175,** 681–682.

Fox, M. J. H., 1976: On the nonlinear transfer in the peak of a gravity-wave spectrum: Part 2. *Proc. Roy. Soc. London*, **A348,** 467–483.

Hasselmann, K., 1962: On the non-linear energy transfer in a gravity-wave spectrum. Part 1: General theory. *J. Fluid Mech.*, **12,** 481–500.

——, 1971: Determination of ocean wave spectra from Doppler ratio return from the sea surface. *Nature*, **229,** 16–17.

——, D. B. Ross, P. Müller and W. Sell, 1976: Parametric wave prediction model. *J. Phys. Oceanogr.*, **6,** 200–228.

——, T. P. Barnett, E. Bouws, H. Carlson, D. E. Cartwright, K. Enke, J. A. Ewing, H. Gienapp, D. E. Hasselmann, P. Kruseman, A. Meerburg, P. Müller, D. J. Olbers, K. Richter, W. Sell and H. Walden, 1973: Measurements of wind-wave growth and swell decay during the Joint North Sea Wave Project. *Deut. Hydrogr. Z.*, Suppl., **A8,** No. 12.

Hidy, G. M., and E. J. Plate, 1966: Wind action on water standing in a laboratory channel. *J. Fluid Mech.*, **26,** 651–687.

Lake, B. M., and H. C. Yuen, 1978: A new model for nonlinear wind waves. Part 1: Physical model and experimental evidence. *J. Fluid Mech.*, **88,** 33–62.

Masuda, A., Y. Y. Kuo and H. Mitsuyasu, 1979: On the dispersion relation of random gravity waves. 1. The framework. *J. Fluid Mech.*, **97,** 717–730.

Mitsuyasu, H., 1968: On the growth of the spectrum of wind-generated waves. *Rep. Res. Inst. Appl. Mech. Kyushu U.*, **16,** 459–482.

——, Y. Y. Kuo and A. Masuda, 1978: The dispersion relation for wind waves in decay area. *Turbulent Fluxes Through the Sea Surface, Wave Dynamics and Prediction*, A. Favré and K. Hasselmann, Eds., Plenum Press, 221–233.

——, —— and ——, 1979: On the dispersion relation of random gravity waves. 2. An experiment. *J. Fluid Mech.*, **97,** 731–749.

Phillips, O. M., 1977: *The Dynamics of the Upper Ocean*, 2nd ed. Cambridge University Press, 336 pp.

——, 1978: Strong interactions in wind-wave fields. *Turbulent Fluxes Through the Sea Surface, Wave Dynamics and Prediction*, A. Favré and K. Hasselmann, Eds., Plenum Press, 373–384.

Ramamonjiarisoa, A., and M. Coantic, 1976: Loi expérimentale de dispersion des vagues produites par le vent sur une faible longueur d'action. *C.R. Acad. Sci. Paris*, **282B,** 111–114.

——, and J.-P. Giovanangeli, 1978: Observations de la vitesse de propagation des vagues engendrées par le vent au large. *C.R. Acad. Sci. Paris*, **287B,** 133–136.

——, S. Baldy and I. Choi, 1978: Laboratory studies on wind-wave generation, amplification and evolution. *Turbulent Fluxes Through the Sea Surface, Wave Dynamics and Prediction*, A. Favré and K. Hasselmann, Eds., Plenum Press, 403–420.

Tick, L. J., 1959: A nonlinear random model of gravity waves. I. *J. Math. Mech.*, **8,** 643–651.

——, 1963: Nonlinear probability models of ocean waves. *Ocean Wave Spectra*, Prentice Hall, 163–170.

Webb, D. J., 1978: Non-linear transfers between sea waves. *Deep-Sea Res.*, **25,** 279–298.

Yefimov, V. V., Y. P. Solov'yev and G. N. Khristoforov, 1972: Observational determination of the phase velocities of spectral components of wind waves. *Izv. Acad. Sci. USSR Atmos. Ocean. Phys.*, **8,** 246–251.